Identification of the conduction-band photoemission in time-resolved two-photon photoemission spectroscopy of Si surfaces

T. Ichibayashi and K. Tanimura
The Institute of Scientific and Industrial Research, Osaka University, 8-1 Mihogaoka, Ibaraki, Osaka 567-0047, Japan
(Received 26 April 2007; published 27 June 2007)

We study photoemissions from Si(111)-(7×7) and Si(001)-(2×1) surfaces by means of time-resolved two-photon photoemission spectroscopy. The peak from the conduction-band minimum (CBM) of bulk Si electronic states has been identified unambiguously in the photoemission spectra for both surfaces, together with peaks from their intrinsic surface states. The CBM photoemission is excited selectively by *p*-polarized probe light with photon energy of around 5 eV. In terms of the one-step model of photoemission, we conclude that the CBM photoemission results from the transition to evanescent final states induced by the surface photoelectric effect.

DOI: 10.1103/PhysRevB.75.235327 PACS number(s): 79.60.Bm, 73.20.−r, 78.47.+p

I. INTRODUCTION

Carrier dynamics on semiconductor surfaces is of great scientific and technological interest. In particular, the dynamics on Si surfaces has been studied extensively using ultrafast optical spectroscopy techniques.[1–12] These studies have revealed ultrafast primary processes of carrier-carrier (*e*-*e*) scattering and electron-phonon (*e*-*p*) scattering. Combined with carrier diffusion[2] and drift transport induced by transient space charging,[1] these processes govern carrier scattering into surface states and hence surface carrier dynamics. In spite of accumulating fundamental knowledge, no clear picture of the ultrafast dynamical coupling of bulk electrons to intrinsic Si surface states has yet emerged.

In the Si(001)-(2×1) surface, which is the basis for most semiconductor devices, rows of asymmetric Si surface dimers form two distinct surface electronic bands: a filled dangling-bond band (D_{up}) and an empty band (D_{down}).[14] The energetics of these intrinsic surface states has been established precisely in a two-photon photoemission (2PPE) spectroscopy study,[6] and furthermore, Weinelt *et al.* have reported the important characteristics of ultrafast relaxation *within* the surface electronic states at low temperatures using time-resolved 2PPE.[11] Additionally, Tanaka and Tanimura reported an excitation-density-dependent electron population transfer to the normally unoccupied D_{down} band at room temperature,[8] without providing a dynamical mechanism due to the lack of information on bulk-electron dynamics. In the other typical reconstructed surface of Si(111)-(7×7), characterized by the dimer-adatom-stacking fault model,[15] adatom dangling bonds form occupied (S_1) and unoccupied (U_1) surface bands.[14] The carrier dynamics on the Si(111)-(7×7) surface has been studied recently by Mauerer *et al.*[12] A broad photoemission band with ultrashort lifetimes has been ascribed to the decay of the temporally occupied U_1 band, and energy-dependent decay characteristics have been analyzed in terms of a surface two-dimensional metallic system. However, the possible roles of bulk hot electrons in the dynamics of electron population into U_1 have not been studied. Thus, relaxation of hot electrons in the bulk conduction band, which are formed simultaneously with surface carriers, and their roles in bulk-to-surface electron transfer remain unclear.

For a comprehensive understanding of the carrier dynamics on semiconductor surfaces in a short temporal domain, it is highly desirable to probe simultaneously both the hot-electron relaxation in the bulk electronic states and the population dynamics of surface electronic states. One of the most powerful methods for such studies is time-resolved 2PPE with femtosecond-temporal resolution,[13] in which probe pulses with photon energies less than the work function are often used to suppress a strong background coming from one-photon photoemission. However, the use of low-photon energy probe light is not typical for studying bulk electronic states in photoemission spectroscopy, and has created some difficulties in measuring the dynamical behavior of bulk electronic states.[13] In the case of Si, in particular, there are no final states available for a momentum-conserving transition up to 7 eV above the conduction-band minimum (CBM).[6,16] Although some previous studies reported photoemission from the CBM of Si in experiments using low probe-photon energies,[2,3] the spectral features were not well characterized and the photoemission process was understood only phenomenologically as "indirect transitions." Therefore, further effort is highly desirable to identify bulk-state photoemission peaks and to elucidate the mechanistic processes of the photoemission in the low-probe-photon-energy regime.

In this paper, we identify definitively the photoemission peak from the CBM in the 2PPE spectra, together with peaks from surface-specific states for Si(001)-(2×1) and Si(111)-(7×7). We conclude that the CBM photoemission is generated by a transition from transiently occupied bulk states near the CBM to an inverse low-energy electron diffraction (LEED) final state with evanescent characteristics. This transition can be induced only by the surface photoelectric effect using probe light with the electric vector perpendicular to the surface. Some spectral features of the CBM peaks are discussed as well.

II. EXPERIMENT

Boron-doped *p*-type Si(001) and Si(111) wafers (10 Ω cm) were clamped with Ta sheets to the sample holder in an ultrahigh vacuum chamber ($<5\times10^{-11}$ Torr). The sur-

face structures were characterized by a scanning tunneling microscope prior to photoemission measurements. The double-domain (2×1) structured surfaces were well ordered for (100) surfaces, with surface-defect concentrations of about 1%. On the other hand, almost perfect (7×7) structures, with surface-defect concentrations less than 0.01%, were prepared for (111) surfaces. Two different laser systems were used in time-resolved 2PPE experiments. A Ti:sapphire oscillator operated with a 76 MHz repetition rate was used to generate 715 nm laser pulses with a temporal width less than 80 fs. Probe pulses of 120 fs width were generated by frequency tripling the oscillator output using nonlinear crystals. Also, in order to excite the surfaces more intensely, a 250 kHz regeneratively amplified Ti:sapphire laser, operated between 745 and 765 nm, was used to pump a tunable optical parametric oscillator and/or amplifier (OPA) to generate pump pulses of 150 fs temporal width and photon energies ranging from 1.8 to 2.6 eV. The probe pulses of 200 fs width were generated by frequency tripling the regenerative amplifier output using nonlinear crystals. The pump and probe pulses, with a preset time delay (Δt), were aligned coaxially and focused on the sample surfaces at 45° to normal. The polarization of pump pulses was chosen to be *s* or *p* polarized, while the polarization of the probe pulses could be set at an arbitrary angle, without changing the temporal and spectral characteristics of the third-harmonic femtosecond-probe pulses. Electrons emitted along the surface normal (±2°) were analyzed by a hemispherical analyzer with an energy resolution of 70 meV.

III. EXPERIMENTAL RESULTS

Under thermal equilibrium, the Fermi level E_F at the Si(111)-(7×7) surface is pinned about 0.7 eV (from 0.63 to 0.78 eV in Ref. 14) above the valence-band maximum (VBM), thus inducing surface band bending. The spurious influence of the surface photovoltage complicates the interpretation of the assignment of photoemission peaks because of its own dynamical behavior.[12,17] Therefore, to make the energetic analysis clear and to avoid effects that distort photoelectron energy distributions, it is essential to perform photoemission measurements under a flatband condition, which can be achieved under intense photoexcitation via the photovoltaic effect.[14] We first measured the photoemission spectra only using probe pulses, with sufficiently weak intensity, illuminating (7×7) surfaces with cw-laser light from another Ti:sapphire laser (800 nm) at different intensities to obtain flatband conditions. We found that downward band bending under thermal equilibrium, or in the dark, is 0.38 ± 0.02 eV at 296 K in a *p*-type specimen with doping concentration of 5×10^{14} cm^{-3} (E_F=0.29 eV above the VBM in the bulk). Therefore, the Fermi level is pinned at 0.67 ± 0.02 eV above the VBM on our well ordered 7×7 *p*-type surface (defect concentration less than 0.01%). Using the well established value of the work function Φ_S (4.60 eV) for Si(111)-(7×7),[14] we calculate the ionization potential ξ for the surface to be 5.27 ± 0.02 eV, which agrees well with the value reported previously for clean Si(111)-(7×7).[18]

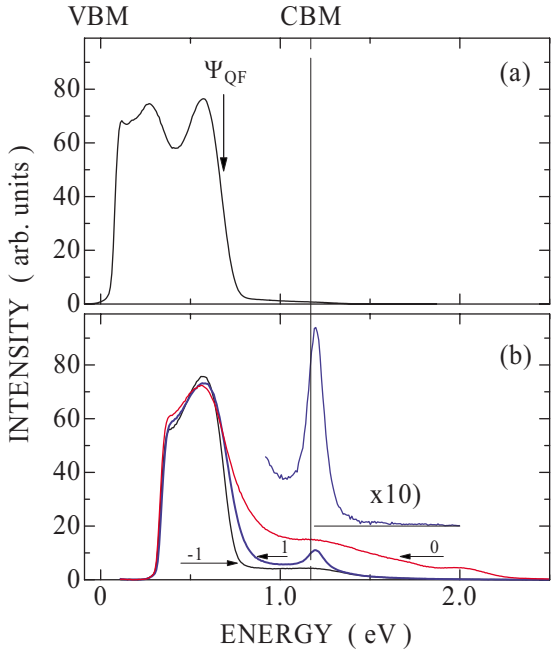

FIG. 1. (Color online) (a) The photoemission spectrum measured with *p*-polarized 5.20 eV femtosecond-probe light for *p*-type Si(111)-(7×7) at 90 K under cw-laser illumination at 800 nm that establishes the flatband condition. The symbol Ψ_{QF} represents the position of the quasi-Fermi-level for the flatband condition. (b) The time-resolved 2PPE spectra for Si(111)-(7×7) at 90 K under excitation with *p*-polarized 2.21 eV pump pulses and probed with *p*-polarized 4.95 eV probe pulses. The curves labeled as −1, 0, and 1 show the spectra measured at probe-time delay (Δt) of −1.0, 0, and 1 ps, respectively. The inset shows the spectrum at $\Delta t=1$ ps in an expanded scale. The spectrum at $\Delta t=-1$ ps is subtracted as a background. In both figures, the energy scale is set with respect to the VBM. The vertical line shows the position of the CBM with the band gap of 1.17 eV.

Based on the basic results described above, we performed 2PPE measurements on Si(111)-(7×7) at 90 K since a persistent flatband condition is more easily attained at low temperatures.[12,19] Figure 1(a) displays the photoemission spectrum measured for the probe-photon energy $(h\nu_p)$ of 5.20 eV under cw-laser illumination that has established flatband condition. Using the values of Φ_S and ξ mentioned above and the Fermi level evaluated for our specimens at 90 K, we can set the energy scale precisely with respect to the VBM (or vacuum level Φ_{vac}). Based on the band-gap energy (1.17 eV) of Si at this temperature, the position of the CBM is set precisely in the abscissa of Fig. 1(a).

For $h\nu_p$=5.20 eV, the low-energy cutoff (E_{cut}) of the spectrum corresponds to the state located 0.07 eV above the VBM. The probe-light intensity was decreased to reduce the two-photon photoemission component, although this component could not be entirely eliminated as indicated by the weak peak above 0.85 eV; the photoemission intensities above 0.85 eV were proportional to the square of the probe-light intensity. Except for the probe-pulse induced two-photon photoemission component, the observed spectrum is located entirely within the band gap of Si. The spectrum represents the intrinsic occupied adatom dangling-bond band

(S_1), since the surface-defect concentration is very small (less than 0.01%). Since the density of states of U_1 extends to the CBM,[20] the high-energy cutoff of the spectrum is characterized by the quasi-Fermi-level Ψ_{QF}, shown by an arrow in the figure, for the light-induced flatband condition. In fact, the shape of the high-energy cutoff could be fitted well by the Fermi distribution function with an effective temperature of 275 K, which is higher than the crystal temperature (90 K). The high electron temperature is characteristic of the nonequilibrated electron distribution under the flatband condition characterized by Ψ_{QF}.

In Fig. 1(b), we show time-resolved 2PPE spectra under excitation by *p*-polarized femtosecond-laser pulses at 2.21 eV generated by our OPA laser. In this measurement, the probe-photon energy is 4.95 eV, which can probe any occupied and transiently occupied states lying more than 0.32 eV above the VBM; E_{cut} is higher than the case in Fig. 1(a) by 0.25 eV with respect to the VBM. Except the difference in E_{cut}, the spectrum at negative delay times, which represents the spectrum prior to excitation, is essentially the same as that in Fig. 1(a), thus confirming the flatband condition even under femtosecond-laser pulse excitation. The carriers generated by a pump pulse establish the flatband condition and maintain it until the arrival of the next pulse.[12] Although the two-photon component above 0.85 eV is more pronounced in Fig. 1(b) than in Fig. 1(a), due to the greater intensity of the probe pulse, the two-photon component is constant for a given probe-pulse intensity. Therefore, this can be regarded as "background" for spectra measured at positive time delays. The spectrum measured at $\Delta t=0$, shown by the curve labeled as 0, is characterized by two features: one is the depression of the intensities below Ψ_{QF} and the other is the significant enhancement of the intensity above Ψ_{QF}. The broad photoemission component for energies above the CBM (well above Ψ_{QF}) shows a fast temporal response, which is essentially the same as the cross-correlation trace between pump and probe pulses. Therefore, they are ascribed to coherent two-photon photoemission. On the other hand, the spectrum measured at $\Delta t=1$ ps (curve labeled as 1), where we can neglect the pump- and probe-pulse overlap, shows one persistent peak at 1.19 eV, which just coincides with the energy position of the CBM. The observed slight high-energy shift of the peak from the precise CBM position is due to the electron distribution near the CBM and the limited energy resolution of our analyzer, as shown in the next section. This photoemission peak can be detected at Δt's greater than 100 ps.

In Fig. 2(a), we show similar results for Si(001)-(2×1) at 296 K. Because of the acceptor characteristic of surface defects, the flatband condition is established for *p*-type Si(001)-(2×1) as demonstrated in Ref. 11. The spectrum measured with $h\nu_p=5.20$ eV can be scaled directly without consideration of possible band-bending effects. Based on the reported values of Φ_S, the ionization energy ξ (=5.40±0.03 eV),[6] and the Fermi level of the present specimens, we can set a precise energy scale with respect to the VBM. The low energy cutoff in this figure corresponds to 0.20 eV above the VBM. In contrast to Si(111)-(7×7), the photoemission intensities below the CBM in the spectrum,

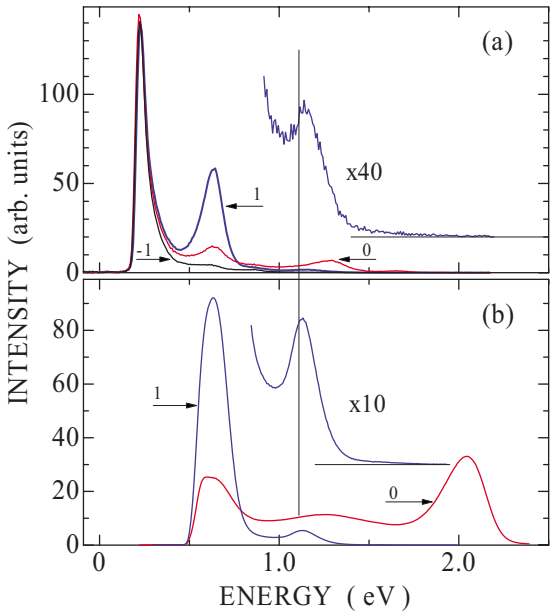

FIG. 2. (Color online) (a) The time-resolved 2PPE spectra measured with *p*-polarized 5.20 eV probe pulses and *p*-polarized 1.73 eV pump pulses for a *p*-type Si(001)-(2×1) at 296 K. The curves labeled as −1, 0, and 1 show the spectra measured at probe-time delay (Δt) of −1.0, 0, and 1 ps, respectively. The inset shows the spectrum at $\Delta t=1$ ps in an expanded scale. The spectrum at $\Delta t=-1$ ps is subtracted as a background. (b) The time-resolved 2PPE spectra for Si(001)-(2×1) at 296 K under excitation with *p*-polarized 2.21 eV pump pulses and probed with *p*-polarized 4.86 eV probe pulses. The curves labeled as 0 and 1 show the spectra measured at probe-time delay (Δt) of 0 and 1 ps, respectively. The spectrum at $\Delta t=-1$ ps is subtracted as a background. The inset shows the spectrum at $\Delta t=1$ ps in an expanded scale. In both figures, the energy scale is set with respect to the VBM. The vertical line shows the position of the CBM with the band gap of 1.12 eV at 296 K.

measured using only the probe laser, are mostly due to surface-defect levels within the band gap, since the intrinsic occupied surface state (D_{up}), located 0.15 eV below the VBM,[6] cannot be probed by 5.2 eV photons.

We also show the 2PPE spectra measured at $\Delta t=0$ ps and 1 ps using *p*-polarized 1.73 eV femtosecond-laser pump pulses. In the spectrum for $\Delta t=0$ ps, the peak at 0.64 eV (electron energy E_K measured from E_{cut} is 0.44 eV) is due to the normally unoccupied state D_{down} at $\bar{\Gamma}$ (the bottom of D_{down}) transiently populated by pump pulses.[8,11] The peak at 1.27 eV ($E_K=1.07$ eV) is the coherent two-photon photoemission associated with the $n=1$ image state resonance with binding energy $E_b=0.69\pm0.05$ eV on this surface.[11,21] The measured electron energy of 1.07 eV agrees reasonably well with the energy evaluated by $h\nu_p-E_b$. In the spectrum for $\Delta t=1$ ps, it appears that the D_{down} peak dominates. However, there is a weak but clearly distinguishable peak at 1.14 eV, which coincides energetically with the CBM (1.12 eV above the VBM at 296 K), as shown in Fig. 2 (expanded scale). Figure 2(b) shows the 2PPE spectra, measured with *p*-polarized 2.21 eV OPA generated pump pulses and 4.86 eV probe pulses. Because of the smaller $h\nu_p$ compared

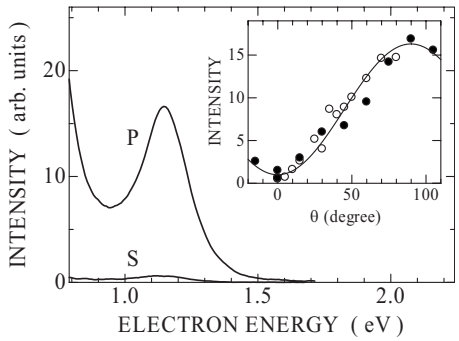

FIG. 3. The 2PPE spectra for Si(001)-(2×1) at 296 K, pumped with *p*-polarized 2.21 eV pump pulses and probed with *p*- and *s*-polarized 4.86 eV probe pulses at a probe-pulse delay of 1 ps. The inset shows the intensity at 1.14 eV peak as a function of polarization angle θ of probe light for Si(111)-(7×7), the filled circles, and for Si(001)-(2×1), the open circles at 296 K. The solid curve shows the probe-light field component perpendicular to the surface, evaluated by $\sin^2\theta$.

to that in Fig. 2(a), the E_{cut} is 0.54 eV above the VBM. In the spectrum measured at $\Delta t=0$ ps, the peak at 2.05 eV ($E_K=1.51$ eV) is the coherent two-photon photoemission associated with the $n=1$ image state resonance, and the growing D_{down} peak is detected at 0.64 eV. The broad peak around 1.3 eV is a coherent two-photon photoemission component, the origin of which will be discussed in a separate paper.[22] In the spectrum at $\Delta t=1$ ps, the peak located at the CBM position is clearly visible without an expanded scale, since the excitation density is about 100 times larger than that used to obtain the results presented in Fig. 2(a). Nonetheless, we plotted the peak by taking the difference between the spectra at $\Delta t=1$ ps and $\Delta t=-1$ ps, with an expanded scale to show the same spectral shape as in Fig. 2(a). Therefore, the photoemission peak, the peak energy of which coincides with the CBM, is detected clearly irrespective of the excitation wavelength and intensity for Si(001)-(2×1).

To further clarify the excitation conditions that induce the CBM peak, we examined the dependence of the spectral intensity on the polarization states of the pump and probe lasers. In Fig. 3, we show the 2PPE spectra measured with *p*- or *s*-polarized probe laser at $\Delta t=1$ ps for Si(001)-(2×1) at 296 K. The 2.21 eV pump laser in this case is *s* polarized. The figure clearly shows that the intensity of the CBM peak, similar to the case of the surface D_{down} peak, is reduced to practically zero for an *s*-polarized probe laser; i.e., we measure a strong probe-light polarization dependence. The same results were obtained for *p*-polarized 2.21 eV pump pulses. A similar strong probe-light polarization dependence has been observed for the CBM photoemission from Si(111)-(7×7) at both 296 and 90 K, thus demonstrating that the polarization effect is not temperature dependent. The inset of Fig. 3 summarizes the probe-light polarization dependence of the CBM-peak intensity for both Si(001)-(2×1) and Si(111)-(7×7) at 296 K; the measured intensity is plotted as the angle θ of probe-laser polarization with respect to the vertical direction of the sample surface; $\theta=0°$ (90°) corresponds to *s* (*p*) polarization. For a given polarization angle θ of the probe light, we evaluated the field component normal to the surface, which is proportional to $\sin^2\theta$, and compare it (solid curve in the inset) with the measured CBM-peak intensities. The polarization-angle dependence of the CBM-peak intensity is well described by this field component. Therefore, only the electric vector perpendicular to the surface can generate the CBM peak. This strong polarization dependence of the CBM-peak intensity provides important information for determining the mechanism that produces the photoemission peak in the present 2PPE measurements.

IV. DISCUSSION

As described previously, a photoemission peak is generated at the energy position precisely at the CBM for both Si(001)-(2×1) and Si(111)-(7×7) excited with pump pulses. Since it is detected at a large Δt, where temporal overlap between pump and probe pulses is negligible, the emission results from transiently occupied real states. The electronic structures of both surfaces have been extensively studied both experimentally and theoretically,[14] and this body of knowledge has shown that there are no such surface states that coincide energetically with the bottom of the bulk conduction band. Therefore, at least energetically, the peak can be ascribed to photoemission from the CBM. Some issues need clarification to establish this conclusion.

The CBM in Si lies along Γ-*X* line at the wave vector (k_{CBM}) of $0.8\times(2\pi/a)$. Therefore, it is projected to $\bar{\Gamma}$ of the surface Brillouin zone of (001) surfaces and can be detected as photoemission along the surface normal. However, theoretical band calculations show that there are no such final states at least 7 eV above the CBM at k_{CBM}.[2,6,16] Therefore, direct optical transitions by the present probe light (ranging from 4.85 to 5.20 eV) are not possible to any final states located above Φ_{vac}. Indirect optical transitions, assisted by phonons, could be possible to states lying above ~5 eV that satisfy the energy conservation with respect to the probe-photon energy.[6,16] However, the state reached by such transitions has an inappropriate symmetry (Δ_5) for generating surface normal emission; the final state must be totally symmetric (Δ_1) for (001) surfaces.[6,23]

The situation becomes more complex for (111) surfaces, since the CBM, lying along the Γ-*X* direction, cannot be projected at $\bar{\Gamma}$ of the surface Brillouin zone of the (1×1) unit cell. However, it is transferred to near $\bar{\Gamma}$ of one of the (7×7) unit cells in terms of surface reciprocal-lattice vectors. Therefore, the momentum requirements could be fulfilled in terms of a backfolded scheme in the (7×7) unit cell or in terms of the surface umklapp process. However, we cannot solve the energy conservation discrepancy for optical transitions from the CBM to any possible final states, as in the case of (001) surfaces. Thus, the traditional model of bulk photoemission fails to describe the photoemission from the CBM for probe light with $h\nu_p\sim5$ eV. Hence, we need to discuss the photoemission process of the CBM peak in the present 2PPE technique in terms of a more precise modeling of photoemission which includes surface photoelectric effects.

Extensive theoretical works were published to describe the photoemission process in terms of the one-step

model.[24–30] Feibelman and Eastman formulated the photoemission from an independent-electron solid in terms of a Green's function formalism.[26] According to their theory, the surface-normal photoemission intensity is governed by the transition from an ensemble of occupied (or transiently occupied) states $\psi_j(\vec{x})$ at a position $\vec{x}$ with energy E_j to the inverse LEED state $\phi_>(\vec{x};\vec{n};E)$, induced by the operator $\hat{O}(\vec{x})$ defined by

$$\hat{O}(\vec{x}) = (1/2)\{\vec{A}(\vec{x}) \cdot \vec{p} + \vec{p} \cdot \vec{A}(\vec{x})\}, \quad (1)$$

with the vector potential $\vec{A}(\vec{x})$ and the electron momentum $\vec{p}$. The vector $\vec{n}$ in $\phi_>(\vec{x};\vec{n};E)$ specifies surface-normal emission. For crystals with bulk three-dimensional periodicity and surface two-dimensional periodicity, both $\psi_j(\vec{x})$ and $\phi_>(\vec{x};\vec{n};E)$ are expressed as linear combinations of propagating and evanescent Bloch functions.[26] For well defined crystalline Bloch states, the dipole approximation of $\hat{O}(\vec{x})$ is often used to specify the initial and final states of photoemission.[23] However, in the present case of photoemission from the CBM, we do not have appropriate final states as discussed above. Therefore, *p*-polarized induced CBM photoemission has no correlations with symmetry selection rules in the optical transitions between bulk Bloch states.

We presume the strong polarization-dependent effect on the CBM photoemission to be a manifestation of the surface photoelectric effect,[29] which has been studied extensively for metals. The surface photoelectric effect includes two contributions, in principle. One comes from nonperiodicity of the crystal potential $V_S(\vec{x})$ near the surface region, characterized by $\partial V_S(z)/\partial z$ along the distance z perpendicular to the surface, and the other is the rapid spatial variation of the longitudinal component of $\vec{A}(\vec{x})$ in a crystal along z. Since the latter contribution is significant only near the plasma frequency ω_p,[29] it is negligible in the present case; the excited density is less than 10^{18} cm^{-3}, and $\hbar\omega_p$ of 16 eV for bulk Si is far above $h\nu_p \sim 5$ eV. Therefore, the classical surface photoelectric effect characterized by $\partial V(z)/\partial z$ is responsible for the observed CBM photoemission.

The Fourier transform of $V_S(z)$ has every component allowed in the bulk periodicity, since $V_S(z)$ is not periodic. Therefore, it couples crystal states having different momentum components k_z normal to the surface. Then, k_z need not be conserved for Bloch states, although $\vec{k}_{\|}$, the wave vector parallel to the surface, must be conserved. Then, in the two-dimensional plane-wave representation for normal emission,[26] $\phi_>(\vec{x};\vec{n};E)$ is expressed as

$$\phi_> = \sum_{\vec{g}} \exp(i\vec{g} \cdot \vec{\rho}) u_{\vec{g}}(z;\vec{n},E), \quad (2)$$

where $\vec{g}$ represents two-dimensional reciprocal-lattice vectors, the vector $\vec{\rho}$ is confined within the two-dimensional periodic surface, and $u_{\vec{g}}(z;\vec{n},E)$ represents the wave function as a function of z for surface-normal emission at energy E. In view of the absence of appropriate final states for photoemission in the energy range concerned, the inverse LEED state may be composed mainly of evanescent wave functions for crystals, which have finite amplitudes only near the surface.

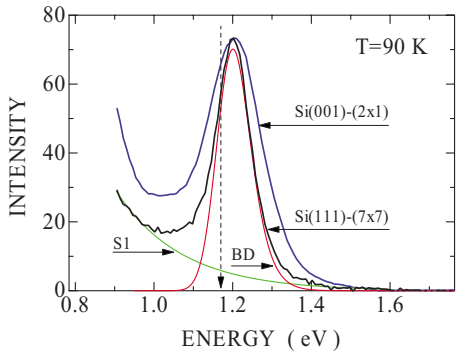

FIG. 4. (Color online) Comparison of spectral shapes of the photoemission peaks associated with the CBM for Si(111)-(7×7) and for Si(001)-(2×1), measured at a sample temperature of 90 K. The curve labeled as S1 shows an extrapolation of the tail of S_1 surface peak and the curve labeled as BD is the Boltzmann distribution function with effective temperature of 300 K, convoluted with 70 meV energy resolution. The broken arrow shows the position of the CBM with the band gap of 1.17 eV at 90 K.

Therefore, even if momentum conservation is weakened by the classical surface photoeffect, the photoemission yield of the CBM peak is small, although the density of transiently occupied CBM states is much larger than that of the surface states. In fact, as seen in Figs. 2 and 3, the CBM-peak intensity is much smaller than the surface peaks, S_1 of Si(111)-(7×7) and D_{down} of Si(001)-(2×1).

Due to final states with evanescent features, we probe the electron population near the CBM only near the surface. Therefore, we can study electron transfer from bulk-to-surface states directly, without concern for transport effects in the bulk. For carriers excited by ~2 eV photons, diffusion out of the short probe region (<10 Å), due to an evanescent contribution from the inverse LEED state, is expected to be slow (>10^{-9} s).[2] This illustrates the special advantage of using time-resolved 2PPE to study surface carrier dynamics on Si. However, some caution should be used when quantitatively analyzing the CBM peak.

In Fig. 4, we compare the CBM spectral shapes measured under the same pump and probe conditions for two different surfaces at the same temperature (90 K). It is clear that the peak width for Si(001) is substantially wider than that for Si(111), although the peak energies are almost identical. To be more quantitative, we analyzed the spectral shape by using a classical electron distribution function for the conduction band, convoluted with our 70 meV energy resolution (under the restriction of sufficiently low excitation density). By subtracting the tail component of the strong S_1 peak, the CBM peak of Si(111)-(7×7) at Δt=1 ps is fitted well by the distribution function using an effective temperature of 300±30 K (the broken curve), which is close to the temperature we obtained by analyzing the quasi-Fermi level in Fig. 1(a). However, the spectral shape for Si(001)-(2×1) could be fitted only by using a significantly higher effective temperature of 650 K.

Precise determination of the inverse LEED function for a given surface requires extensive theoretical work, as has been carried out for other surfaces.[27,28] However, it is pre-

sumed that for the two different surfaces we studied, the states may comprise different wave functions $u_{\vec{g}}(z;\vec{n},E)$'s in Eq. (2) since both $\vec{n}$ and $\vec{g}$ are different. Also, the magnitudes of $\partial V_S(z)/\partial z$ and the components k_z's involved are different for different surfaces. Therefore, even if we assume constant transmission amplitude from an inverse LEED state to free electron vacuum states, in a narrow energy range, the spectral shape of CBM emission may not be the same. Also, since the concentration of surface defects on Si(001)-(2×1) is greater than that on Si(111)-(7×7), the broader width might come from the surface defects due to momentum-conserved relaxation parallel to the surface. Therefore, direct comparison of physical quantities obtained from spectral shape analysis between different surfaces may not prove meaningful. However, the time-resolved 2PPE technique allows us to study the role of ultrafast hot-electron dynamics of bulk-to-surface transitions for a given surface by simultaneously probing both the relaxation dynamics of hot electrons in the bulk conduction band and population dynamics of surface-specific electronic states. The results of such studies on Si surfaces will be published elsewhere.[31]

V. SUMMARY

The photoemission peak from the conduction-band minimum of Si can be clearly detected in time-resolved 2PPE spectra with probe-photon energies of approximately 5 eV. It has been shown that the surface photoelectric effect induces the photoemission by exciting the transiently populated electrons at the CBM to the inverse LEED states, which have evanescent features in this energy range. Therefore, time-resolved 2PPE can probe hot-electron dynamics both in bulk- and surface electronic states simultaneously leading to much more comprehensive understanding of ultrafast carrier dynamics on Si surfaces.

ACKNOWLEDGMENTS

We wish to thank Th. Fauster and U. Höfer for important discussion and valuable comments. This work was supported by a Grant-in-Aid for Scientific Research from the Ministry of Education, Science, Technology, Sports, and Culture of Japan.

[1] N. J. Halas and J. Bokor, Phys. Rev. Lett. **62**, 1679 (1989).
[2] M. W. Rowe, H. Liu, G. P. Williams, Jr., and R. T. Williams, Phys. Rev. B **47**, 2048 (1993).
[3] J. R. Goldman and J. A. Prybyla, Phys. Rev. Lett. **72**, 1364 (1994).
[4] T. Sjodin, H. Petek, and H. L. Dai, Phys. Rev. Lett. **81**, 5664 (1998).
[5] S. Jeong and J. Bokor, Phys. Rev. B **59**, 4943 (1999).
[6] C. Kentsch, M. Kutschera, M. Weinelt, Th. Fauster, and M. Rohlfing, Phys. Rev. B **65**, 035323 (2001).
[7] A. J. Sabbah and D. M. Riffe, Phys. Rev. B **66**, 165217 (2002).
[8] S. Tanaka and K. Tanimura, Surf. Sci. **529**, L251 (2003).
[9] M. Hase, M. Kitajima, A. M. Constantinescu, and H. Petek, Nature (London) **426**, 51 (2003).
[10] C. Voelkmann, M. Reichelt, T. Meier, S. W. Koch, and U. Höfer, Phys. Rev. Lett. **92**, 127405 (2004).
[11] M. Weinelt, M. Kutschera, Th. Fauster, and M. Rohlfing, Phys. Rev. Lett. **92**, 126801 (2004); Appl. Phys. A: Mater. Sci. Process. **A80**, 995 (2005).
[12] M. Mauerer, I. L. Shumay, W. Berthold, and U. Höfer, Phys. Rev. B **73**, 245305 (2006).
[13] *Solid-State Photoemission and Related Methods: Theory and Experiment*, edited by W. Schattke and W. A. Van Hove (Wiley-VCH, GmbH & Co., 2003).
[14] W. Mönch, *Semiconductor Surfaces and Interfaces* (Springer, Berlin, 1995).
[15] K. Takayanagi, Y. Tanimshiro, M. Takahashi, and S. Takahashi, J. Vac. Sci. Technol. A **3**, 1502 (1985); Surf. Sci. **164**, 367 (1985).
[16] C. S. Wang and B. M. Klein, Phys. Rev. B **24**, 3393 (1981).
[17] J. P. Long, H. R. Sadeghi, J. C. Rife, and M. N. Kabler, Phys. Rev. Lett. **64**, 1158 (1990).
[18] G. Hollinger and F. J. Himpsel, J. Vac. Sci. Technol. A **1**, 640 (1983).
[19] J. E. Demuth, W. J. Thompson, N. J. DiNardo, and R. Imbihl, Phys. Rev. Lett. **56**, 1408 (1986).
[20] Th. Fauster and F. J. Himpsel, J. Vac. Sci. Technol. A **1**, 1111 (1983).
[21] M. Kutschera, M. Weinelt, M. Rohlfing, and T. Fauster, Appl. Phys. A: Mater. Sci. Process. (to be published).
[22] T. Ichibayashi and K. Tanimura (unpublished).
[23] W. Eberhardt and F. J. Himpsel, Phys. Rev. B **21**, 5572 (1980).
[24] G. D. Mahan, Phys. Rev. B **2**, 4334 (1970).
[25] W. Schaich and N. W. Ashcroft, Phys. Rev. B **3**, 2452 (1971).
[26] P. J. Feibelman and D. E. Eastman, Phys. Rev. B **10**, 4932 (1974).
[27] A. Liebsch, Phys. Rev. Lett. **32**, 1203 (1974).
[28] J. B. Pendry, Surf. Sci. **57**, 679 (1976).
[29] E. W. Plummer and W. Eberhardt, Adv. Chem. Phys. **49**, 533 (1982).
[30] H. J. Levinson, E. W. Plummer, and P. J. Feibelman, Phys. Rev. Lett. **43**, 952 (1979).
[31] T. Ichibayashi, S. Tanaka, and K. Tanimura (unpublished).